Characterizing the Random Positioning Machine: Guidelines for Expanded Use as a Reduced-gravity Analog

Anna Wadhwa, Lasse Bruun, Johan CG Petersen, Lonnie Petersen

Supplementary Information (SI) Appendix

Supplementary Equation S1: Centripetal acceleration
Supplementary Equation S2: Coriolis acceleration
Supplementary Equation S3: Euler acceleration
Supplementary Equations S4-15: Three-Frame RPM Kinematics Model

Supplementary Figure S1: Drifting during RPM rotation
Supplementary Figure S2: Additional examples of pole bias in a two-frame RPM
Supplementary Figure S3: Some control algorithms have no pole bias but do not cover the entire desired gravity trajectory

Supplementary Video S1: Motion capture recording of the random positioning machine (RPM) at ω_I = 12°/s and ω_O = 24°/s
Supplementary Video S2: Motion capture recording of the random positioning machine (RPM) at ω_I = 18°/s and ω_O = 24°/s.

Supplementary Equation (S1): $\alpha_{centripetal} = \varpi \times (\varpi \times \bar{P})$
Where $\bar{P}$ is the vector from the center of rotation to point P

Supplementary Equation (S2): $\alpha_{Coriolis} = 2\varpi \times V_{moving\ frame}$
Where V is velocity vector in m/s

Supplementary Equation (S3): $\alpha_{Euler} = \dot{\varpi} \times \bar{P}$

Three-Frame RPM Kinematics Model:
G = global static reference
O = outer RPM frame
M = middle RPM frame
I = inner RPM frame
τ = Angle between frames G and O
σ = Angle between frames O and M
θ = Angle between frames M and I
And additional variables (e.g., R, P, α_G) as defined in the two-frame model (see main manuscript text)

We first define angular velocity:
(S4) $\varpi_G = \varpi_O + R_{G,O} \cdot \varpi_M + R_{G,O} R_{O,M} \cdot \varpi_I$

We then define the angular acceleration for each individual frame (O, M, I):
(S5) $\varpi_G = \varpi_O + R_{G,O} \cdot \varpi_M + R_{G,O} R_{O,M} \cdot \varpi_I$
(S6) $[\dot{\varpi}_O]_G = [\dot{\varpi}_O]_O + [\varpi_O \times (\varpi_O)] = [\dot{\varpi}_O]_O$
(S7) $[\dot{\varpi}_M]_G = (R_{G,O} \cdot [\dot{\varpi}_M]_O) + [\varpi_O \times (R_{G,O} \cdot \varpi_M)]$
(S8) $[\dot{\varpi}_I]_G = (R_{G,M} \cdot [\dot{\varpi}_I]_O) + [\varpi_O \times (R_{G,O} \cdot \varpi_M) \times (R_{G,M} \cdot \varpi_I)]$

These can be combined into one expression for the global reference (G):
(S9) $\alpha_G = \dot{\varpi}_G = [\dot{\varpi}_O]_G + [\dot{\varpi}_M]_G + [\dot{\varpi}_I]_G$

As defined for the two-frame RPM model, we must also incorporate additional accelerations when considering a point P on the platform:
(S10) $\alpha_{G,P} = \alpha_G + \alpha_{O,P} + \alpha_{G,P(centripetal)} + \alpha_{G,P(Coriolis)} + \alpha_{G,P(Euler)}$
(S11) $\alpha_{O,P} = \alpha_M + \alpha_{M,P} + \alpha_{O,P(centripetal)} + \alpha_{O,P(Coriolis)} + \alpha_{O,P(Euler)}$
(S12) $\alpha_{M,P} = \alpha_I + \alpha_{I,P} + \alpha_{M,P(centripetal)} + \alpha_{M,P(Coriolis)} + \alpha_{M,P(Euler)}$

Converting these to the G frame (e.g., subscript *M,G* would mean calculating in the M frame and converting to the G frame using the rotational matrices):
(S13) $[\alpha_{O,P}]_G = [\alpha_{M,P}]_G + [\varpi_{O,M} \times (\varpi_{O,M} \times \bar{P}_{O,I})]_{O,G} + [2\varpi_{O,M} \times (\varpi_{M,P} \times \bar{P}_{M,P})]_{O,G} + [\dot{\varpi}_{O,M} \times \bar{P}_{O,I}]_{O,G}$
(S14) $[\alpha_{M,P}]_G = [\varpi_{M,I} \times (\varpi_{M,I} \times \bar{P}_{M,I})]_{O,G} + [\dot{\varpi}_{M,I} \times \bar{P}_{M,I}]_{M,G}$

Finally, we can determine the total acceleration on a point P fully in terms of the static global reference. Therefore, $\alpha_{G,P}$ is dependent on the rotational rates of all frames and location of point P on the platform:
(S15) $\alpha_{G,P} = \alpha_G + [\alpha_{O,P}]_G + [\varpi_{O,G} \times (\varpi_{O,G} \times \bar{P}_{G,I})] + [2\varpi_{G,O} \times (\varpi_{M,P} \times \bar{P}_{M,P}) \times (\varpi_{O,P} \times \bar{P}_{O,P})] + [\dot{\varpi}_{O,G} \times \bar{P}_{G,I}]$

Supplementary Figure S1: Drifting during RPM rotation.

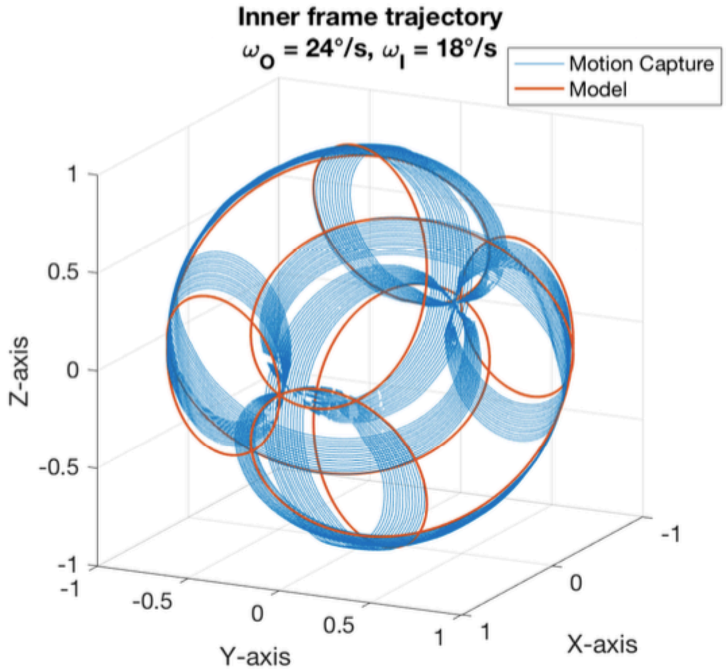

Motion capture trajectory of a point P on an RPM does not align with the ideal kinematics model due to RPM drifting. This happens when the rotational rate achieved by the RPM is unable to match that specified by the user.

Supplementary Figure S2: Additional Examples of Pole bias in a two-frame RPM.

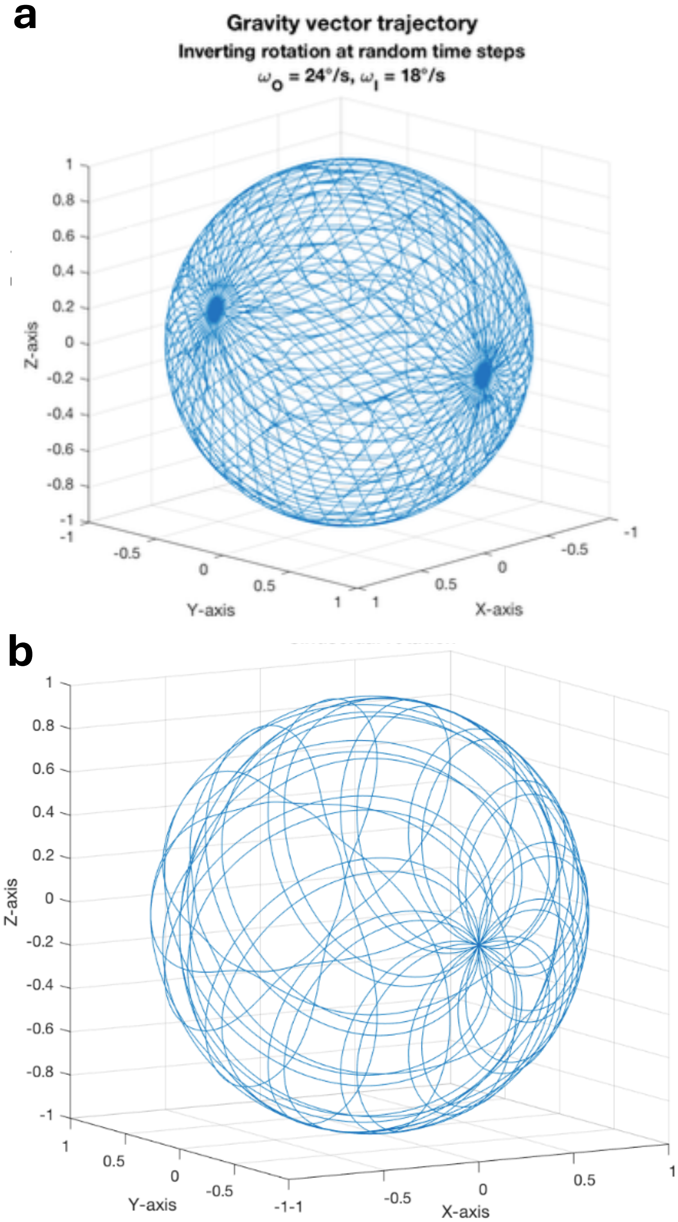

A) *Demonstration of pole bias in the cumulative trajectory of the gravity vector after 50 minutes with constant ω_O = ±24 deg/s and ω_I = ±18 deg/s. Direction was randomly changed every 30-60 seconds. RPM was allowed 2 seconds to reach the new rotational rate.* ***B)*** *Trajectory of the gravity vector is shown after 1hr of rotation with a sinusoidal function that does not allow a full rotation of the outer frame.*

Supplementary Figure S3: Some control algorithms have no pole bias but do not cover the entire desired gravity trajectory.

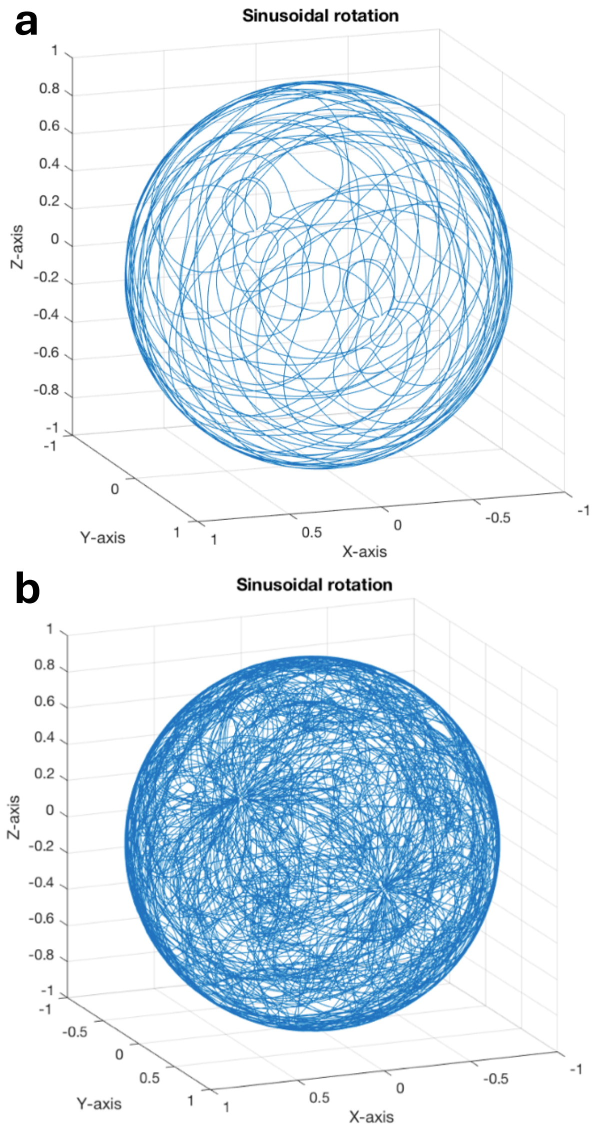

*Trajectory of the gravity vector is shown after 3 hrs of sinusoidal rotation of the outer frame and **A)** constant rotation of the inner frame or **B)** randomly changing the rotation of the inner frame in the range from 2 to −2 rev/min. Pole bias is not present but the trajectory path does not cover the entire unit sphere even after 3 hours of rotation.*

Supplementary Video S1: Motion capture recording of the RPM at ω_I = 12°/s and ω_O = 24°/s. Full link to view online: https://youtu.be/u8mcWJt7FeA

Supplementary Video S2: Motion capture recording of the RPM at ω_I = 18°/s and ω_O = 24°/s. Full link to view online: https://youtu.be/2jlCe653H4s